

Supporting Information

Mirpour and Bisley 10.1073/pnas.1120763109

SI Results

Behavioral Fit Justification. We used a combination of a hyperbolic discount function (Eq. 3) combined with a logistic function (Eq. 2) to fit the behavioral data. According to the behavior (points, Fig. 1 *B–E*) it was clear that changing the number of potential targets and the number of distractors changed the probability of choosing a target (T). Given that rewards were linked to Ts, this can be thought of as a change in the probability of receiving a reward for a T. The hyperbolic function we used to describe subjective value (Eq. 3) is often thought of in regards to dealing with delayed outcomes (1, 2); however, it is now well established that it is appropriate for choices with probabilistic outcomes (3, 4). In fact, Green and Myerson (5) have suggested that the same (or similar) underlying processes might account for both probability and temporal discounting. Therefore, we used this hyperbolic function to calculate subjective value as a function of the number of objects. The outcome of this function is essentially a discount value, although we were not able to explicitly test this given the constraints of our task. To correlate the difference in values with the choice of the monkeys, we used a logistic function (Eq. 2). This function has been used before to go from subjective value to choice in both monkeys (1) and human subjects (6, 7). In our hands, these functions fit the data incredibly well.

Before finalizing which functions we would use, we tested many alternatives. To test whether our function indeed described our data better, we calculated AIC_C (corrected Akaike Information Criterion) values for the various one-, two-, and three-parameter functions. The difference between the smallest AIC_C value, which came from the three-parameter function, and the AIC_C values for the one- and two-parameter functions were very large for both monkeys. Therefore, the likelihood of getting a better fit with a one- or two-parameter function was essentially zero. Of the three-parameter functions we tested, the one presented in Eq. 2 gave us the most reliable fits in both animals and allowed us to extract three useful measures of value: the predicted probability of fixating any object in a specific stimulus class, the subjective value of any object in a specific stimulus class, and the preference for objects in that stimulus class over objects in other classes.

Cross-Validation Control. There is a possibility that the strong correlation between the calculated downstream responses and the behavior (Fig. 4 *A* and *B*) is the result of overfitting the function to the behavioral data. To test this possibility we ran a cross-validation control in which the functions were fitted to the data over 1,000 iterations. In each iteration, 75% of fixations within a single session were used as a training set, and the remaining fixations were used as the validation set. Specifically, once all fixations were characterized according to the number of Ts and the number of distractors, the fixations in each category were randomly assigned into either the training or validation set for each iteration. The behavioral functions were fit to the training set, and the parameters of the fit were extracted. Then the predicted probabilities of making a saccade to a T were calculated for the validation set. The predicted probabilities of the validation set were then compared with the observed ones. All iterations showed significant correlations, with a mean correlation coefficient of 0.89 and SD of 0.12 (Fig. S4 *A* and *B*). On the basis of the fit parameters of each iteration, the correlation between the calculated downstream response to a T and the preference for that stimulus was also calculated. In this analysis, all iterations showed significant correlations, with a mean correlation coefficient of 0.86 and SD of 0.06 (Fig. S4 *C* and *D*). The

strong significant range of correlations in the cross-validation tests confirm that the strong correlation between neural data and the preference is not the result of overfitting particular functions to a particular data set.

This analysis can also be used to interpret the robustness of the behavioral fits in estimating the preference. For example, even though the cross-validation of the behavioral fits of monkey D produced a wide range of correlations (Fig. S4*A*), the fit parameters consistently made a series of strong correlations between calculated downstream response and the preference (Fig. S4*C*). We can infer from these results that the variance of the behavioral fit parameters (and eventually the preference) was small enough to generate a couple of clusters of strong correlations between the preference and the calculated downstream response in each animal.

We can also use the output from this analysis to show that the relationship between the calculated downstream response and stimulus preference is better than the relationship between calculated downstream response and the actual behavior. Fig. 2 *E* and *F* show the relationship between calculated downstream response and the observed probability of fixating any T, our metric of the animals' saccade goal selection. The correlation coefficients from these two fits are both significantly less than the mean correlation coefficients from the cross-validation analyses comparing stimulus preference to calculated downstream response (Fig. S4 *C* and *D*; $P \ll 0.001$, one-sample *t* tests).

Shuffle Correlation Analysis. There is a possibility that the source of all or part of the correlation between stimulus preference and the calculated downstream response might be the use of the number of targets (N_T) and the number of distractors (N_D) in calculating both stimulus preference and calculated downstream response. To investigate this possibility we ran a series of shuffle correlation analyses to see how much of the correlation is contributed by an actual relationship and how much of it is due to the common factors. In this analysis we calculated the preference to potential targets, fixated Ts and Ds for each fixation separately using the fit variables obtained in the original analysis (shown in the bottom two rows of Table S1). As in that analysis, we determined the mean numbers of objects to be used in the calculated downstream response formula using all the fixations within a session that had the same preference. However, before plotting the data, we shuffled the neural activity and randomly assigned the responses to a class and then calculated the calculated downstream responses and the correlation between calculated downstream responses and preferences. In this manner the neural activity is randomly assigned to preferences. We repeated this process 1,000 times. Distributions of the correlation coefficients between the calculated downstream response, using the shuffled neural data, and stimulus preference are shown in Fig. S5 *A–F* for each category of stimulus and monkey separately. The original correlation coefficients (Fig. 5 *C–H*) are shown by the inverted triangles and do not lie within the shuffled distributions (Fig. S5; $P \ll 0.001$, one-sample *t* tests). In each panel, the result of the best correlation from the shuffled data is plotted in the *Inset*. A comparison of these *Insets* with the scatter plots shown in Fig. 5 *C–H* emphasizes that the shuffled correlations were primarily driven by a single region of the graph (usually the left side, with low preference), whereas the actual data are correlated across all preferences. These data suggest that some of the correlation we see between the calculated downstream response and stimulus preference may be due to common factors, but they cannot explain the much higher correlations found in the actual data.

SI Methods

All experiments were approved by the Chancellor's Animal Research Committee at University of California, Los Angeles as complying with the guidelines established in the Public Health Service Guide for the Care and Use of Laboratory Animals.

Surgical Preparation. Two rhesus monkeys (9–12 kg) were implanted with head posts, scleral coils, and recording cylinders during sterile surgery under general anesthesia (8); animals were initially anesthetized with ketamine and xylazine and maintained with isoflurane.

Electrophysiological Recording. Both animals were trained on the standard memory-guided saccade (MGS) and the foraging search tasks. We recorded extracellular single-unit activity from the lateral intraparietal area (LIP) using tungsten microelectrodes guided by coordinates from MRI images. Recorded neurons were considered to be in LIP if they showed the typical pattern of LIP activity, consisting of a visual burst, delayed sustained activity, and/or a peri-saccadic burst, during the MGS task (9). The size and position of the receptive field of each neuron was estimated using an automated MGS task covering 9 or 25 points (see ref. 10 for details). Neurons that did not allow us to have only a single stimulus in the receptive field were rejected.

To begin a trial of the foraging task (Fig. 1A), the monkeys had to fixate on a spot placed to one side of the screen. After a delay of 450–700 ms, an array of potential targets (T) and distractors (+) was presented, with one over the fixation spot. One of the targets had a juice reward associated with it, such that if the monkey looked at it for 500 ms within 8 s after the start of the trial, he would get the reward. As in previous free-viewing visual search studies (8, 11, 12), the stimuli were arranged in such a fashion that when the monkey looked at one stimulus, the receptive field of an LIP neuron encompassed another stimulus. The number of targets and distractors varied in each trial. Although the total number of objects was always equal to or less than 10, the number of potential targets ranged from one to seven, and the number of distractors ranged from zero to seven during behavioral data collection. Only two sets of trials were used during the neural recording sessions. Either the number of potential targets was always three, and the number of objects varied among three, five, or seven, or the total number of objects was always 10, and the number of potential targets varied among three, five or seven.

Data Analysis. Data were recorded from 95 LIP neurons (53 from monkey E and 42 from monkey D). We analyzed neural activity during fixations in which there was a single object inside the receptive field. Data were aligned by the beginning of fixation, and we analyzed the mean spike rates within a 350-ms window starting 150 ms after the end of the last saccade (i.e., the beginning of fixation). We roughly discriminated action potentials online and then accurately sorted spikes offline using SortClient software (Plexon Inc.). The experiments were run using the REX system (13), and data were recorded using the Plexon system (Plexon Inc.). Data were analyzed using custom code written in MATLAB (Mathworks).

Exponential choice functions (Eqs. 2 and 5) were fit to the behavioral data using a weighted nonlinear regression technique. For the fitting of the behavioral data, the observed probabilities were calculated by pooling all fixations across all sessions, in which the same number of object classes were present (e.g., three potential targets, two fixated Ts, and five distractors), and calculating the probability of making a saccade to any stimulus in each of the three classes. For the initial analysis, calculated downstream responses were calculated according to the number of Ts, distractors, and the average neural responses to Ts and distractors in that condition. These responses were plotted against the behavior or the estimates of value (saccade probability, stimulus preference, and subjective value) calculated from those conditions using the fit variables obtained in the original fit (Table S1).

For the analyses in which we included three classes of stimuli, the observed probabilities were used to fit the behavioral data (Eq. 5) and to give values to our four fit variables (β , K_T , k_{JT} , and K_D ; Table S1). Because of the limited number of trials in any given condition in a single session, the data plotted in Fig. 5 came from averaging across trials with different numbers of objects, but similar preferences, within a session. This was accomplished by using the three relevant fit variables to calculate an estimate of preference for each fixation. Within each session, there were a limited number of unique preferences, so all trials with these unique preferences were pooled and the mean number of potential targets, fixated Ts, and distractors calculated from these trials. These mean numbers of stimuli were used with the actual mean responses for each class of stimulus to calculate the calculated downstream response for this set of data within a single session.

1. Louie K, Glimcher PW (2010) Separating value from choice: Delay discounting activity in the lateral intraparietal area. *J Neurosci* 30:5498–5507.
2. Mazur JE (1987) *Quantitative Analyses of Behavior: The Effect of Delay and of Intervening Events on Reinforcement Value*, eds Commons ML, Nevin J, Rachlin H (Erlbaum, Hillsdale, NJ), Vol 5, pp 55–73.
3. Prelec D, Loewenstein G (1991) Decision making over time and under uncertainty: A common approach. *Manage Sci* 37:770–786.
4. Rachlin H, Raineri A, Cross D (1991) Subjective probability and delay. *J Exp Anal Behav* 55:233–244.
5. Green L, Myerson J (2004) A discounting framework for choice with delayed and probabilistic rewards. *Psychol Bull* 130:769–792.
6. Kable JW, Glimcher PW (2007) The neural correlates of subjective value during intertemporal choice. *Nat Neurosci* 10:1625–1633.
7. Levy I, Snell J, Nelson AJ, Rustichini A, Glimcher PW (2010) Neural representation of subjective value under risk and ambiguity. *J Neurophysiol* 103:1036–1047.
8. Mirpour K, Arcizet F, Ong WS, Bisley JW (2009) Been there, seen that: A neural mechanism for performing efficient visual search. *J Neurophysiol* 102:3481–3491.
9. Barash S, Bracewell RM, Fogassi L, Gnadt JW, Andersen RA (1991) Saccade-related activity in the lateral intraparietal area. I. Temporal properties; comparison with area 7a. *J Neurophysiol* 66:1095–1108.
10. Mirpour K, Ong WS, Bisley JW (2010) Microstimulation of posterior parietal cortex biases the selection of eye movement goals during search. *J Neurophysiol* 104:3021–3028.
11. Bichot NP, Rossi AF, Desimone R (2005) Parallel and serial neural mechanisms for visual search in macaque area V4. *Science* 308:529–534.
12. Mazer JA, Gallant JL (2003) Goal-related activity in V4 during free viewing visual search. Evidence for a ventral stream visual salience map. *Neuron* 40:1241–1250.
13. Hays AV, Richmond BJ, Optican LM (1982) Unix-based multiple-process system, for real-time data acquisition and control. *WESCON Conf Proc* 2:1–10.

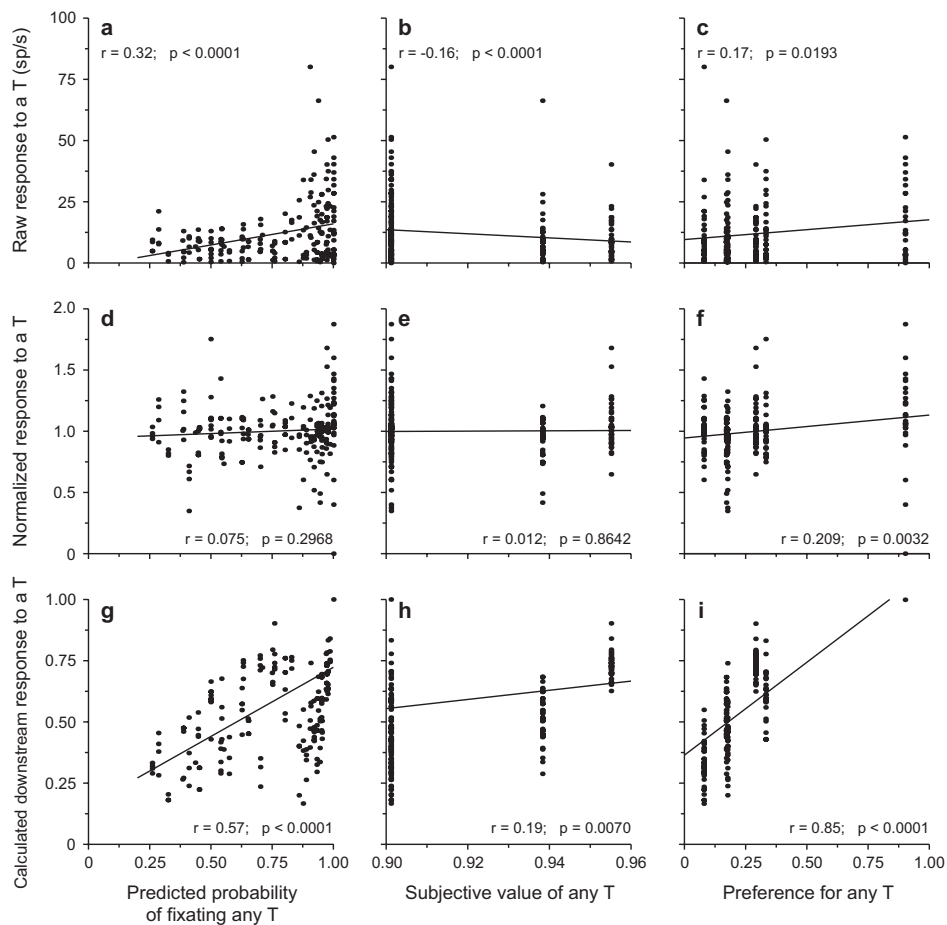


Fig. S3. Relationship between LIP activity and our estimates of value for monkey E. Each point in each panel represents the response of one neuron in one condition, whereby a condition is defined by the number of potential targets and number of distractors present in the array. All estimates of value were obtained using the fit shown in Fig. 3B and with the parameters listed in the second row of Table S1. Raw responses (*Top*), normalized responses (*Middle*), and calculated downstream responses (*Bottom*) to potential targets (T) are plotted against the probability of fixating any T (*A*, *D*, and *G*), the subjective value of any T (*B*, *E*, and *H*), and the preference for any T (*C*, *F*, and *I*). Black lines represent the least square regression lines. Normalized responses were calculated by dividing the response in one condition by the mean response for that neuron under all six conditions.

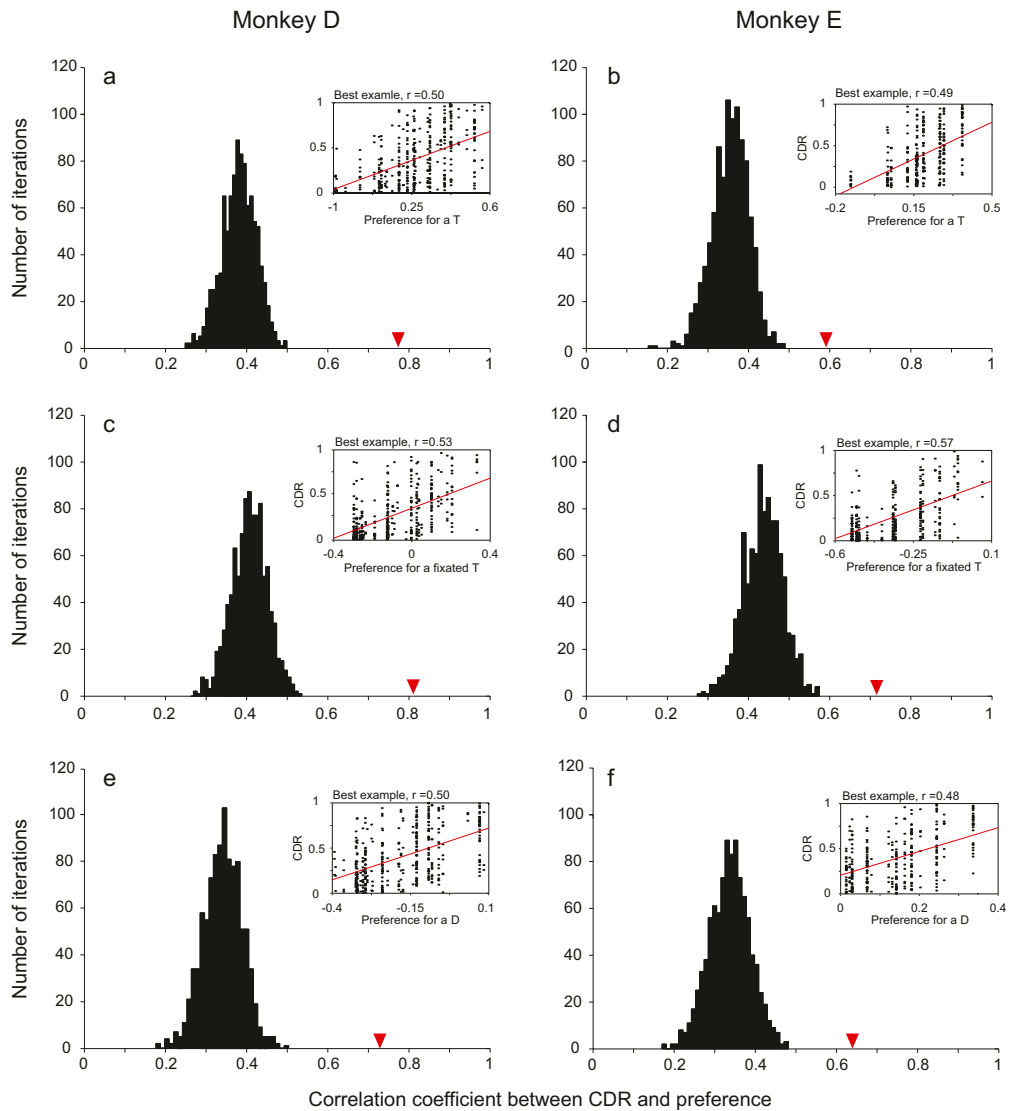


Fig. S5. Shuffle correlation analysis. Distribution of the correlation coefficients between calculated downstream response (CDR) and the stimulus preferences using 1,000 iterations of shuffled average neural responses to potential targets (A and B), fixated Ts (C and D), and distractors (E and F) plotted separately for monkeys D and E. *Insets:* Best examples from each distribution are plotted. Red triangles represent the correlation coefficients from the actual data (from Fig. 5 C–H).

